Semi-local Total Variation for Regularization of Inverse Problems

Laurent Condat

Semi-local Total Variation for Regularization of Inverse Problems

Laurent Condat

***Abstract*— We propose the discrete semi-local total variation (SLTV) as a new regularization for inverse problems in imaging. We show that the corresponding optimization problems can be efficiently solved by a primal-dual algorithm, which is easy to implement. The SLTV favors piecewise linear images, so that the main drawback of the total variation, its clustering effect, is avoided.**

***Index Terms*— total variation, non-local regularization, inverse problems, convex optimization, primal-dual splitting, proximal operator**

I. Introduction

We investigate the use of a regularization functional which extends the popular total variation with non-local correlation terms, for the problem of image denoising and beyond it, to handle general inverse problems of imaging. Indeed, many image processing problems can be formalized as the recovery of an image $u = (u[\mathbf{k}])_{\mathbf{k}\in\mathbb{Z}^2}$ from noisy linear measurements

$$b = \mathcal{A}u + \varepsilon \tag{1}$$

where ε is a realization of noise. The linear operator $\mathcal{A}$ typically accounts for some blurring or sub-sampling so that the recovery of u from b is an ill-posed inverse problem. One classical way to seek a solution is to rely on regularization. That is, we solve the variational problem

$$\hat{u} = \operatorname*{argmin}_v \mathcal{J}(v) + \frac{\lambda}{2}\|\mathcal{A}v - b\|^2, \tag{2}$$

where the parameter λ controls the tradeoff between the fit to the data and the prior knowledge that $\mathcal{J}(u)$ is small for the class of images considered. We can note that the choice of the best value of λ given b and the noise variance is a problem by itself [1]–[3].

When there is no noise, some problems, typically interpolation problems, require to solve

$$\hat{u} = \operatorname*{argmin}_v \mathcal{J}(v) \quad \text{s.t.} \quad \mathcal{A}v = b. \tag{3}$$

We note that the minimizer of (2) or (3) is not necessarily unique, depending on the kernel of the operator $\mathcal{A}$.

Tikhonov regularization consists in choosing the quadratic penalty $\mathcal{J}(v) = \|\nabla v\|_{\ell_2}^2$, which yields a linear solution. The drawback of this simple model is over-smoothing of the textures and edges for natural images. Another popular penalty is (isotropic) total variation (TV), first introduced for denoising in [4] and then applied to many inverse problems [5]. In the discrete setting,

$$\mathcal{J}_{\mathrm{TV}}(v) = \|\nabla v\|_{\ell_1} = \sum_{\mathbf{k}\in\mathbb{Z}^2} \|\nabla v[\mathbf{k}]\|_2 \tag{4}$$

with

$$\nabla v[\mathbf{k}] = \big[v[k_1+1,k_2] - v[\mathbf{k}], v[k_1,k_2+1] - v[\mathbf{k}]\big]^{\mathrm{T}}. \tag{5}$$

and $\|\mathbf{a}\|_2 = \sqrt{|a_1|^2 + |a_2|^2}$. Note that boldface letters denote vectors throughout the paper, e.g. $\mathbf{k} = [k_1, k_2]^{\mathrm{T}} \in \mathbb{Z}^2$. TV regularization yields images with sharp edges but the textures are still over-smoothed, there are staircasing effects and the pixel values in smooth regions are clustered in piecewise constant areas, which gives an unpleasant synthetical look to the reconstructed images.

To overcome the drawbacks of methods based on the interactions of local pixel values solely, non-local methods have become increasingly popular. Nonlocal image denoising based on patch-distances was proposed by Buades *et al.* [6]. This non-local averaging shares similarities with patch-based computer graphics synthesis [7], [8]. Non-local filtering can be understood as a quadratic regularization based on a non-local graph [9]–[11]. This quadratic regularization can be extended to non-smooth energies such as the TV on graphs, which has been defined over the continuous domain by Gilboa *et al.* [12] and over the discrete domain by Zhou and Schölkopf [13]. Elmoataz *et al.* [14] consider a larger class of non-smooth energies involving a p-laplacian for $p < 2$.

Expressed in the discrete setting, the non-local functional of Gilboa *et al.* [12], [15] can be written as

$$\mathcal{J}_{\mathrm{NL}}(v) = \sum_{\mathbf{k}\in\mathbb{Z}^2} \sum_{\mathbf{l}\in\mathbb{Z}^2} \phi(|v[\mathbf{k}] - v[\mathbf{l}]|) w(\mathbf{k},\mathbf{l}) \tag{6}$$

for a positive convex function ϕ. The positive and symmetric weight function $w(\mathbf{k},\mathbf{l})$ can be understood as the proximity of the image features at locations $\mathbf{k}$ and $\mathbf{l}$. Its choice is critical. It can be obtained based on patch distances like in the Non-local means denoising method, from a first estimate of the image u obtained by solving (2) with Tikhonov regularization; or it can be defined implicitely from the geometry of v and updated iteratively at the same time as the solution [16].

In this work, we focus instead on a functional similar to (6) but based on gradient differences instead of pixel values differences and without the introduction of the weight function, which is difficult to determine. The functional is as follows:

$$\mathcal{J}_{\mathrm{SLTV}}(v) = \sum_{\mathbf{k}\in\mathbb{Z}^2} \sum_{\mathbf{l}\in\mathbb{Z}^2 \,|\, \mathbf{l}-\mathbf{k}\in\Omega} \|\nabla v[\mathbf{k}] - \nabla v[\mathbf{l}]\|_2 \tag{7}$$

L. Condat is with the Image Team of the GREYC laboratory, a joint CNRS-UCBN-ENSICAEN research unit in Caen, France. Contact: see http://www.greyc.ensicaen.fr/∼lcondat/.

for some set of pixels $\Omega \subset \mathbb{Z}^2$. $\mathcal{J}_{\mathrm{SLTV}}$ is semi-local, since the gradient is compared to other gradients in its neighborhood. This functional was proposed and studied in the continuous domain by Kindermann *et al.* [17], as a semi-local extension of the total variation. Since $\mathcal{J}_{\mathrm{SLTV}}(v) = 0$ if v represents an affine function, it is expected that the minimization of $\mathcal{J}_{\mathrm{SLTV}}$ will favor piecewise affine functions over piecewise constant ones, avoiding staircasing. This has been confirmed by experiments in [17].

In this work, we propose an efficient method to solve the problems (2) and (3) with $\mathcal{J} = \mathcal{J}_{\mathrm{SLTV}}$, to exploit the potential of this functional and show that it provides superior performances over the total variation. In [17], the computation was done by an explicit Euler method for the steepest descent flow of the problem (2). It is known that this optimization approach is particularly slow. Moreover, in [17], $\|\mathbf{a}\|_2$ is replaced by $\sqrt{a_1^2 + a_2^2 + \beta}$ for a small $\beta > 0$ in the expression (7), to make the problem (2) differentiable. To solve (2) with $\mathcal{J} = \mathcal{J}_{\mathrm{NL}}$ and in the specific case of denoising ($\mathcal{A} = \mathcal{I}d$) Gilboa and Osher in [15] extended the dual algorithm developed by Chambolle for TV denoising [18]. A split-Bregman approach was also developed in [19]. However, these methods cannot be extended to the case of inverse problems with $\mathcal{A} \neq \mathcal{I}d$. In [16], a forward-backward splitting method is introduced to solve (2) with $\mathcal{J} = \mathcal{J}_{\mathrm{NL}}$, but this is an iterative method with a non-local denoising problem to solve at each iteration, which is computationally expensive. Recently, a breakthrough in the field of convex optimization has appeared under the form of new primal-dual methods proposed independently by several authors [20]–[22]. To our knowledge, the primal-dual framework of Chambolle *et al.* [20] outperforms all other methods when solving (2) or (3) with $\mathcal{J}_{\mathrm{TV}}$ [5], [20]. In this work, we show that this primal-dual framework is particularly adequate to solve (2) or (3) with the functional $\mathcal{J}_{\mathrm{SLTV}}$ and an arbitrary operator $\mathcal{A}$. We detail the new algorithms in Sect. II and show some examples of applications in Sect. III.

II. A Generic Primal-Dual Algorithm for Semi-Local TV Minimization

The two problems (2) and (3) can both be formulated under the form

$$\hat{u} = \operatorname*{argmin}_v \mathcal{J}(v) + \mathcal{F}_2(v) \tag{8}$$

where $\mathcal{F}_2(v) = \frac{\lambda}{2}\|\mathcal{A}v - b\|^2$ in (2) and $\mathcal{F}_2(v) = \imath_{\mathcal{A}v=b}(v)$ in (3), where we introduce the indicator function of a property $P(v)$ as

$$\imath_{P(v)}(v) = \begin{cases} 0 & \text{if} \quad P(v) \text{ is satisfied} \\ +\infty & \text{else.} \end{cases} \tag{9}$$

$\mathcal{J}$ and $\mathcal{F}_2$ are convex functions, but they are not differentiable, which rules out conventional smooth optimization techniques. Therefore, efficient optimization techniques to solve (8) proceed by *splitting*, in that the functions $\mathcal{J}$ and $\mathcal{F}_2$ are used individually. They are called *proximal* because each nonsmooth function is involved via its *proximity operator*. The proximity operator of a functional $\mathcal{G}$ is defined by

$$\mathrm{prox}_{\mathcal{G}}(x) = \operatorname*{argmin}_y \mathcal{G}(y) + \frac{1}{2}\|x - y\|^2. \tag{10}$$

We refer the reader to the excellent review article [23] for an introduction to proximal splitting methods. The classical splitting methods, like the forward-backward method, can be used to solve (8), but they involve the computation of $\mathrm{prox}_{\mathcal{J}}$, which amounts to solve a denoising problem, at each iteration. Thus, they are computationally expensive. Recently [20], the following generic problem was studied:

$$\hat{u} = \operatorname*{argmin}_v \mathcal{F}_1(\mathcal{K}v) + \mathcal{F}_2(v) \tag{11}$$

for some convex functionals $\mathcal{F}_1$ and $\mathcal{F}_2$ and linear operator $\mathcal{K}$. We define the Fenchel conjugate $\mathcal{G}^*$ of a functional $\mathcal{G}$ by [23]

$$\mathcal{G}^*(x) = \sup_y \langle x, y\rangle - \mathcal{G}(y). \tag{12}$$

Then, the generic algorithm presented in [20] to solve (11) is as follows:

First order primal-dual algorithm

1. Choose $\delta, \tau > 0$ such that $\delta\tau\|\mathcal{K}\|^2 \leq 1$ and the initial estimate $u^{(0)}$, set $\mathbf{a} := (\mathbf{0})_{\mathbf{k}\in\mathbb{Z}^2}$, $\bar{u}^{(0)} := u^{(0)}$, $n := 0$.
2. Iterate until stopping criterion is met
3. $\quad \mathbf{a}^{(n+1/2)} := \mathbf{a}^{(n)} + \delta\mathcal{K}\bar{u}^{(n)}$
4. $\quad \mathbf{a}^{(n+1)} := \mathrm{prox}_{\delta\mathcal{F}_1^*}(\mathbf{a}^{(n+1/2)})$
5. $\quad u^{(n+1/2)} := u^{(n)} - \tau\mathcal{K}^*\mathbf{a}^{(n+1)}$
6. $\quad u^{(n+1)} := \mathrm{prox}_{\tau\mathcal{F}_2}(u^{(n+1/2)})$
7. $\quad \bar{u}^{(n+1)} := 2u^{(n+1)} - u^{(n)}$
8. $\quad n := n + 1$

$u^{(n)}$ converges to a minimizer $\hat{u}$ of (11) as $n \to +\infty$.

Now, the problem (8) with $\mathcal{J} = \mathcal{J}_{SLTV}$ can exactly be recast in the form (11). For this, let $N = |\Omega|$ be the number of pixels in Ω and $\mathbf{m}_1, \ldots, \mathbf{m}_N \in \mathbb{Z}^2$ be the elements of Ω. Then, $\mathcal{K}(v) = \mathbf{a}$ with

$$\mathbf{a}[\mathbf{k}]_i = \nabla v[\mathbf{k}] - \nabla v[\mathbf{k}+\mathbf{m}_i] \in \mathbb{R}^2, \quad \forall \mathbf{k} \in \mathbb{Z}^2,\ \forall i = 1, \ldots, N \tag{13}$$

and

$$\mathcal{F}_1(\mathbf{a}) = \sum_{\mathbf{k}\in\mathbb{Z}^2} \sum_{i=1}^{N} \|\mathbf{a}[\mathbf{k}]_i\|_2. \tag{14}$$

We also have $\mathcal{K}^*(\mathbf{a}) = v$ with, for every $\mathbf{k} \in \mathbb{Z}^2$,

$$\begin{aligned} v[\mathbf{k}] = \sum_{i=1}^{N} & a[k_1 - 1, k_2]_{i,1} - a[\mathbf{k}]_{i,1} - \\ & a[k_1 - m_{i,1} - 1, k_2 - m_{i,2}]_{i,1} + \\ & a[k_1 - m_{i,1}, k_2 - m_{i,2}]_{i,1} + \\ & a[k_1, k_2 - 1]_{i,2} - a[\mathbf{k}]_{i,2} - \\ & a[k_1 - m_{i,1}, k_2 - m_{i,2} - 1]_{i,2} + \\ & a[k_1 - m_{i,1}, k_2 - m_{i,2}]_{i,2}. \end{aligned} \tag{15}$$

Then, we have to make explicit the proximal operators of $\delta\mathcal{F}_1^*$ and $\tau\mathcal{F}_2$. For $\mathcal{F}_2(v) = \frac{\lambda}{2}\|\mathcal{A}v - b\|^2$, it is easy to show that

$$\mathrm{prox}_{\tau\mathcal{F}_2}(v) = (\mathcal{I}d + \lambda\tau\mathcal{A}^*\mathcal{A})^{-1}(v + \lambda\tau\mathcal{A}^*b). \tag{16}$$

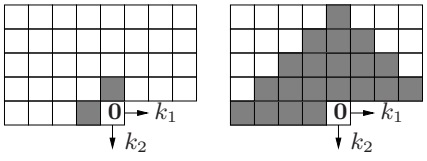

(a) (b)

Fig. 1. In grey, the pixels of the sets Ω_1 (a) and Ω_4 (b).

Note that if $\mathcal{A}\mathcal{A}^* = \mathcal{I}d$, which is the case for some interpolation problems, (16) simplifies to

$$\mathrm{prox}_{\tau\mathcal{F}_2}(v) = (\mathcal{I}d - \frac{\lambda\tau}{1+\lambda\tau}\mathcal{A}^*\mathcal{A})(v + \lambda\tau\mathcal{A}^*b) \quad (17)$$

$$= v + \frac{\lambda\tau}{1+\lambda\tau}\mathcal{A}^*(b - \mathcal{A}v). \quad (18)$$

In the case where it is not convenient to apply the operator $(\mathcal{I}d + \lambda\tau\mathcal{A}^*\mathcal{A})^{-1}$ in (16), it is possible to modify the primal-dual algorithm so that only the operators $\mathcal{A}$ and $\mathcal{A}^*$ are required, see [20, eq. (74)].

When a functional is an indicator function $\imath_P$, its proximity operator is the orthogonal projection onto the set $\{v \mid P(v)\}$. Therefore, when $\mathcal{F}_2(v) = \imath_{\mathcal{A}v=b}(v)$, we have

$$\mathrm{prox}_{\tau\mathcal{F}_2}(v) = v + \mathcal{A}^+(b - \mathcal{A}v), \quad (19)$$

where $\mathcal{A}^+$ is the Moore-Penrose pseudo-inverse of $\mathcal{A}$. If $\mathcal{A}\mathcal{A}^*$ is invertible, then $\mathcal{A}^+ = \mathcal{A}^*(\mathcal{A}\mathcal{A}^*)^{-1}$.

We now determine the proximity operator of $\delta\mathcal{F}_1^*$. For this, we define the property

$$P(\mathbf{a}) \equiv \sup_{\mathbf{k}\in\mathbb{Z}^2} \max_{i=1,\dots,N} \|\mathbf{a}[\mathbf{k}]_i\|_2 \leq 1 \quad (20)$$

Then, we have

$$\imath^*_{P(\mathbf{a})}(\mathbf{a}) = \sup_{\mathbf{b}} \langle \mathbf{a}, \mathbf{b}\rangle - \imath_{P(\mathbf{b})}(\mathbf{b}) \quad (21)$$

$$= \sup_{0<\rho\leq 1} \sup_{\mathbf{b} \mid \sup_{\mathbf{k}\in\mathbb{Z}^2} \max_{i=1,\dots,N} \|\mathbf{b}[\mathbf{k}]_i\|_2 = \rho} \langle \mathbf{a}, \mathbf{b}\rangle \quad (22)$$

$$= \sup_{0<\rho\leq 1} \rho \sum_{\mathbf{k}\in\mathbb{Z}^2} \sum_{i=1}^{N} \|\mathbf{a}[\mathbf{k}]_i\|_2 \quad (23)$$

$$= \sum_{\mathbf{k}\in\mathbb{Z}^2} \sum_{i=1}^{N} \|\mathbf{a}[\mathbf{k}]_i\|_2 = \mathcal{F}_1(\mathbf{a}). \quad (24)$$

Thus, $\imath_P^* = \mathcal{F}_1$. The bi-conjugate relation $\mathcal{G}^{**} = \mathcal{G}$ yields $\delta\mathcal{F}_1^* = \delta\imath_P = \imath_P$. Therefore, $\mathrm{prox}_{\delta\mathcal{F}_1^*}$ is the orthogonal projection

$$\mathrm{prox}_{\delta\mathcal{F}_1^*}(\mathbf{a}) = \mathbf{b} \text{ with } \mathbf{b}[\mathbf{k}]_i = \frac{\mathbf{a}[\mathbf{k}]_i}{\|\mathbf{a}[\mathbf{k}]_i\|_2}, \quad \forall \mathbf{k} \in \mathbb{Z}^2, \forall i = 1, \dots, N \quad (25)$$

The last point to discuss is the choice of the set Ω in the definition of the semi-local TV. We remark that if Ω is symmetric, (7) can be rewritten as

$$\mathcal{J}_{\mathrm{SLTV}}(v) = 2 \sum_{\mathbf{k}\in\mathbb{Z}^2} \sum_{\mathbf{l}\in\mathbb{Z}^2 \mid \mathbf{l}-\mathbf{k}\in\Omega, \mathbf{l}<\mathbf{k}} \|\nabla v[\mathbf{k}] - \nabla v[\mathbf{l}]\|_2, \quad (26)$$

where $\mathbf{l} < \mathbf{k}$ is understood in the lexicographic order. Therefore, we can choose Ω as half of a symmetric set. This is advantageous because the size of the memory buffer for the dual variable $\mathbf{a}$ and the computation time are proportional to the size $N = |\Omega|$ of Ω.

Once Ω has been chosen, we can compute the operator norm $\|\mathcal{K}\|$, which is necessary to choose the time steps δ, τ in the algorithm. We have $\|\mathcal{K}\|^2 = \|\mathcal{K}^*\mathcal{K}\|$ and $\mathcal{K}^*\mathcal{K}$ is a linear shift-invariant operator on images; that is, it corresponds to a convolution: $\mathcal{K}^*\mathcal{K}(v) = v * h$ for some filter h. Hence, $\|\mathcal{K}^*\mathcal{K}\| = \sup_{\boldsymbol{\omega}\in[-\pi,\pi]^2} \hat{h}(\boldsymbol{\omega})$, where $\hat{h}(\boldsymbol{\omega}) = \sum_{\mathbf{k}\in\mathbb{Z}^2} h[\mathbf{k}]e^{-j\boldsymbol{\omega}^{\mathrm{T}}\mathbf{k}}$ is the Fourier transform of h. For the two sets Ω_1 and Ω_4 depicted in Fig. 1, we have $\|\mathcal{K}\|^2 = 64$ and $\|\mathcal{K}\|^2 \approx 325.63$. In all our experiments with $\mathcal{J}_{\mathrm{SLTV}}$, for pixel values in the range $[0, 255]$, we chose $\tau = 0.1$ and $\delta = 1/\|\mathcal{K}\|^2/\tau$.

III. Experimental Examples

A. Denoising

We first consider the denoising problem, with $\mathcal{A} = \mathcal{I}d$. In Fig. 2, four parts of popular test images are shown, along with their noisy versions, where additive white Gaussian noise (AWGN) of standard deviation $\sigma = 20$ has been added. The third row of Fig. 2 shows the denoised images using total variation ($\mathcal{J} = \mathcal{J}_{\mathrm{TV}}$), where the value of λ has been tuned manually to maximize the PSNR, for each image. This optimal value of λ yields images where noise is still visible, while some image details have disappeared, see e.g. the stripes of the pants in image (j). When decreasing further λ to obtain visually better images without remaining noise, even more details are washed out, as shown in the fourth row of the figure. Moreover, the classical drawback of total variation, which is to yield images where the pixel values are clustered into piecewise constant regions, is clearly visible on the face of Barbara, see image (m).

The fifth-eighth row of Fig. 2 show the results with semi-local total variation ($\mathcal{J} = \mathcal{J}_{\mathrm{SLTV}}$). The neighborhood set Ω_1 depicted in Fig. 1 is too small to correctly capture the inter-pixel correlations and a large part of noise remains in images (q)–(t). Much better results are obtained with $\Omega = \Omega_4$. As is visible in images (u)–(x), the tradeoff between noise removing and details preservation is better with SLTV than with TV. When further decreasing λ, as shown in images (y)–(β), we obtain smooth images where the sharpness of the strong edges is maintained, without the clustering and staircasing effects proper to total variation. We found that there is virtually no improvement in choosing a set Ω larger than Ω_4.

B. Zooming

A zooming experiment by a factor 4×4 is shown in Fig. 3 on a part of the Boat image, see Fig. 2 (d). No noise is present, so that we solve (3) where $\mathcal{A}$ is the downscaling operator by averaging over 4×4 blocks. Note that $\mathcal{A}\mathcal{A}^* = \mathcal{I}d/16$. As result, with SLTV, the edges are slightly less sharp than with TV, but the clustering effect of the latter is avoided. Note that both TV and SLTV regularizations suffer from the intrinsic lack of isotropy of the discrete gradient operator (5); thus, in interpolation problems like zooming, the direction $-45°$ is privileged over the direction $45°$ and a directional brushing effect is visible both in Fig. 3 (b) and (c).

original

(a) (b) (c) (d)

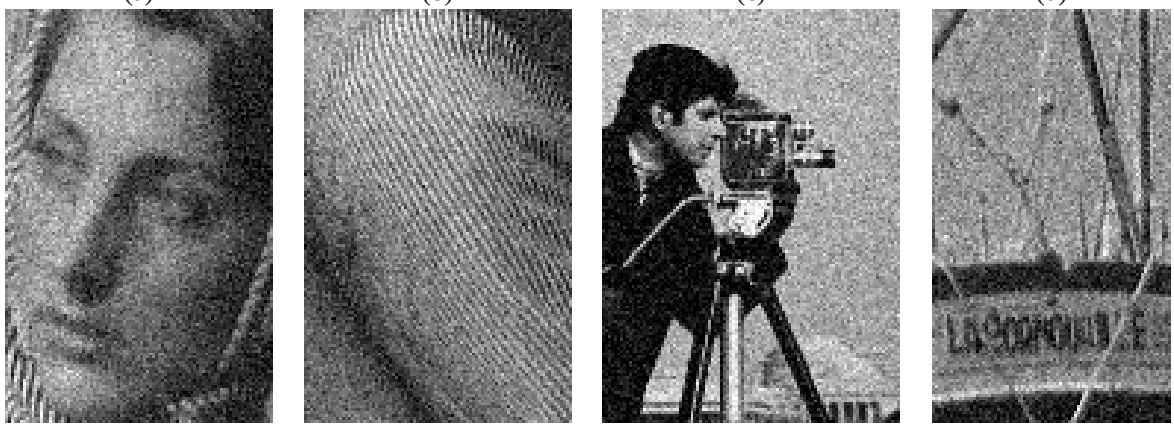

noisy, $\sigma = 20$

(e) (f) (g) (h)

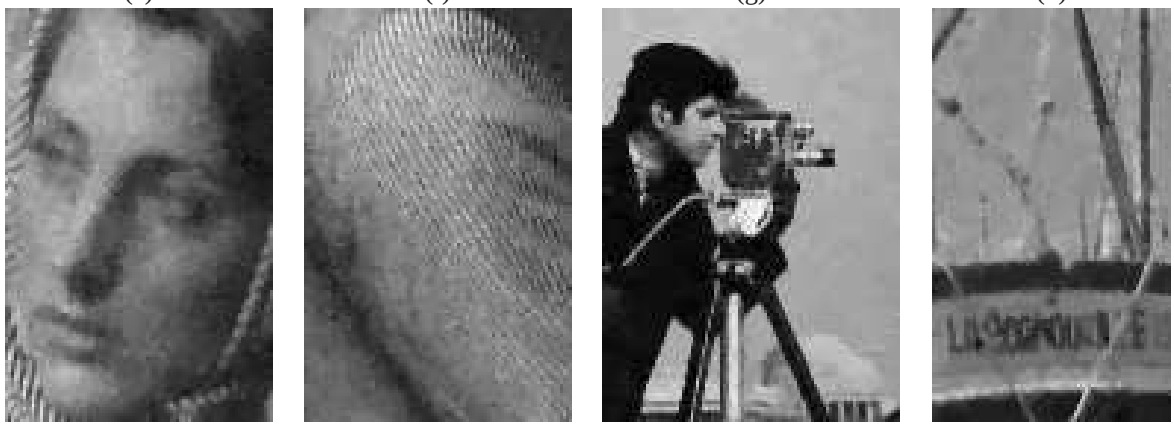

denoised
$\mathcal{J} = \mathcal{J}_{\mathrm{TV}}$
optimal λ

(i) $\lambda = 0.09$, 27.03dB (j) $\lambda = 0.09$, 27.03dB (k) $\lambda = 0.07$, 28.88dB (l) $\lambda = 0.07$, 29.18dB

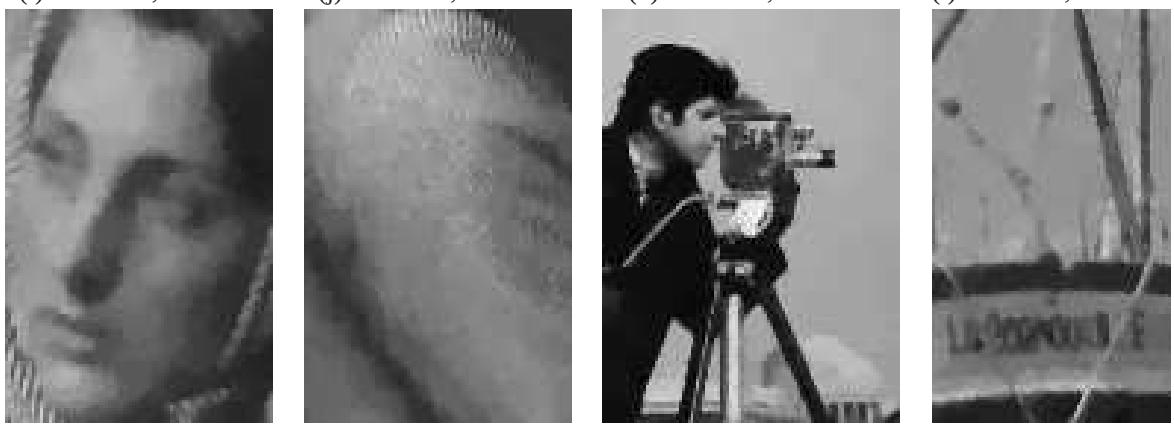

denoised
$\mathcal{J} = \mathcal{J}_{\mathrm{TV}}$
$\lambda = 0.05$

(m) 25.71dB (n) 25.71dB (o) 28.14dB (p) 28.60dB

Fig. 2. Denoising experiments using regularization with total variation and proposed semi-local total variation. For each denoised image, 100 iterations of the primal-dual algorithm were run. The PSNR values correspond to the whole Barbara, Camera and Boat, images, not to the crops selected here.

Fig. 2 (continued).

Fig. 3. Zooming experiment on a part of the Boat Image, by a factor 4×4. (a) by pixel replication (b) by solving (3) with TV. (c) by solving (3) with SLTV. 100 iterations of the primal-dual algorithm were run and the image obtained by pixel replication was used as initial estimate by the algorithm.

C. Demosaicking

Another classical interpolation problem in imaging is demosaicking, which consists in reconstructing a color image $\mathbf{u} = [u_R, u_G, u_B]^{\mathrm{T}}$ with red (R), green (G), blue (B) channels, knowing only one of these three values at each pixel

TABLE I

PSNR (IN DB) FOR THE DEMOSAICKING EXPERIMENTS OVER THE 24 IMAGES OF THE CLASSICAL KODAK TEST SET.

image	TV	SLTV	13	35.75	**36.36**
1	39.20	**39.72**	14	34.95	**36.68**
2	38.24	**39.92**	15	37.99	**39.33**
3	41.32	**42.52**	16	42.31	**42.67**
4	39.19	**40.52**	17	40.08	**41.27**
5	35.95	**37.61**	18	35.88	**37.33**
6	38.72	**39.44**	19	38.74	**39.38**
7	39.78	**42.07**	20	40.09	**41.27**
8	35.00	**35.67**	21	38.82	**39.73**
9	40.80	**42.06**	22	36.85	**38.09**
10	40.41	**41.84**	23	40.80	**42.62**
11	38.00	**39.55**	24	33.26	**34.93**
12	42.38	**43.36**	mean	38.52	**39.75**

location [24]. That is, $\mathcal{A}\mathbf{u} = b$ with $b[\mathbf{k}] = \{u_G[\mathbf{k}]$ if $k_1 + k_2$ is even, $u_R[\mathbf{k}]$ else if k_2 is even, $u_B[\mathbf{k}]$ else$\}$, $\forall \mathbf{k} \in \mathbb{Z}^2$. Note that $\mathcal{A}\mathcal{A}^* = \mathcal{I}d$. In [25], the author proposed an extension of the total variation to color images as follows:

$$\mathcal{J}_{\mathrm{TV}}(\mathbf{u}) = \mu\, \mathcal{J}_{\mathrm{TV}}(u_L) + \mathcal{J}_{\mathrm{TV}}(u_C), \tag{27}$$

where $u_C = u_{G/M} + j.u_{R/B}$ is the complex chrominance field and $u_L, u_{G/M}, u_{R/B}$ are the channels of $\mathbf{u}$ expressed in the luminance, green-magenta and red-blue chrominance orthonormal basis [25]. The parameter $\mu < 1$ in (27) ensures that the reconstructed image has its chrominance channels smoother than its luminance channel, a known property of natural images. It is straightforward to extend the definition of the SLTV to color images using the same definition as the color TV in (27). Like in [25], we can use the primal-dual strategy to minimize the color SLTV, by switching between the representation of a color image in the R,G,B and luminance,chrominance bases.

The results of solving (3) with $\mathcal{J} = \mathcal{J}_{\mathrm{TV}}$ and $\mathcal{J}_{\mathrm{SLTV}}$ are reported in Tab. I. We used $\mu = 0.625$. The large average improvement of 1.2dB obtained with the SLTV over the TV shows that the SLTV is a better regularization for the demosaicking problem.

We can also consider the joint demosaicking-denoising problem for which the mosaicked image is corrupted by AWGN, with std. dev. 20. We solved (2) and illustrate the result in Fig. 4. The visual quality of the images reconstructed with the TV and the SLTV is comparable, but the latter is free from the piecewise constant clustering effect of the TV. Moreover, the SLTV tends to give images with more accurate colors, while with the TV, the colors are desaturated, especially on small objects. This can be seen on the blue rudder in the man's hands, which appears more blue in (c) than in (b).

IV. CONCLUSION

In this article, we proposed the semi-local total variation (SLTV) as an alternative to the total variation (TV) for regularization of inverse problems in imaging. We have shown that the recent primal-dual framework proposed in [20] can be efficiently applied to the minimization of the SLTV. Hence, for a cost of about $|\Omega_4| = 20$ times the cost of the TV minimization, we obtain restored images where piecewise constant areas are favored, instead of the too rough piecewise constant model underlying the TV. Other said, SLTV yields more pleasant images where the sharpness of edges is maintained without the clustering effect which is the main drawback of the TV.

We would like to stress that this work neither aims at giving state-of-the-art results in inverse problems, nor pretends proposing the best optimization strategy to solve the problems. We instead showed how regularization by SLTV can be harnessed easily to a variety of applications, potentially yielding better results than the popular TV.

REFERENCES

[1] S. Ramani, T. Blu, and M. Unser, "Monte-Carlo SURE: A black-box optimization of regularization parameters for general denoising algorithms," *IEEE Trans. Image Processing*, vol. 17, no. 9, pp. 1540–1554, Sept. 2008.

[2] J.-C. Pesquet, A. Benazza-Benyahia, and C. Chaux, "A SURE approach for digital signal/image deconvolution problems," *IEEE Trans. Signal Processing*, vol. 57, no. 12, pp. 4616–4632, Dec. 2009.

[3] R. Giryes, M. Elad, and Y. C. Eldar, "The projected GSURE for automatic parameter tuning in iterative shrinkage methods," *Applied and Computational Harmonic Analysis*, to appear.

[4] L. Rudin, S. Osher, and E. Fatemi, "Nonlinear total variation based noise removal algorithms," *Physica D*, vol. 60, no. 1–4, pp. 259–268, 1992.

[5] A. Chambolle, V. Caselles, D. Cremers, M. Novaga, and T. Pock, "An introduction to total variation for image analysis," in *Theoretical Foundations and Numerical Methods for Sparse Recovery*, vol. 9. De Gruyter, Radon Series Comp. Appl. Math., 2010, pp. 263–340.

[6] A. Buades, B. Coll, and J.-M. Morel, "A review of image denoising algorithms, with a new one," *SIAM Journal on Multiscale Modeling and Simulation*, vol. 4, no. 2, pp. 490–530, 2005.

[7] A. A. Efros and T. K. Leung, "Texture synthesis by non-parametric sampling," in *Proc. of ICCV*, 1999, pp. 1033–1038.

[8] L. Y. Wei and M. Levoy, "Fast texture synthesis using tree-structured vector quantization," in *Proc. of SIGGRAPH*, 2000, pp. 479–488.

[9] R. R. Coifman, S. Lafon, A. B. Lee, M. Maggioni, B. Nadler, F. Warner, and S. W. Zucker, "Geometric diffusions as a tool for harmonic analysis and structure denition of data: Diffusion maps," in *Proc. of the Nat. Ac. of Science*, vol. 102, 2005, pp. 7426–7431.

[10] A. D. Szlam, R. R. Coifman, and M. Maggioni, "A general framework for adaptive regularization based on diffusion processes," *Journ. Mach. Learn. Res.*, vol. 9, pp. 1711–1739, Aug. 2008.

[11] G. Gilboa and S. Osher, "Nonlocal linear image regularization and supervised segmentation," *SIAM Multiscale Modeling and Simulation*, vol. 6, pp. 595–630, 2007.

[12] G. Gilboa, J. Darbon, S. Osher, and T. F. Chan, "Nonlocal convex functionals for image regularization," UCLA CAM, Tech. Rep. Report 06-57, Oct. 2006.

[13] D. Zhou and B. Schölkopf, "Regularization on discrete spaces," in *German Pattern Recognition Symposium*, 2005, pp. 361–368.

[14] A. Elmoataz, O. Lezoray, and S. Bougleux, "Nonlocal discrete regularization on weighted graphs: a framework for image and manifold processing," *IEEE Trans. Image Processing*, vol. 17, no. 7, pp. 1047–1060, 2008.

[15] G. Gilboa and S. Osher, "Nonlocal operators with applications to image processing," *Multiscale Model. Simul.*, vol. 7, no. 3, pp. 1005–1028, 2008.

[16] G. Peyré, S. Bougleux, and L. Cohen, "Non-local regularization of inverse problems," in *Proc. of ECCV*, 2008, pp. 57–68.

[17] S. Kindermann, S. Osher, and P. W. Jones, "Deblurring and denoising of images by nonlocal functionals," *Multiscale Model. Simul.*, vol. 4, no. 4, pp. 1091–1115, 2006.

[18] A. Chambolle, "An algorithm for total variation minimization and applications," *Journal of Mathematical Imaging and Vision*, vol. 20, no. 1–2, pp. 89–97, 2004.

[19] X. Bresson, "A short note for nonlocal TV minimization," Tech. Rep., June 2009.

[20] A. Chambolle and T. Pock, "A first-order primal-dual algorithm for convex problems with applications to imaging," CMAP, Tech. Rep. R. I. 685, May 2010.

[21] E. Esser, X. Zhang, and T. Chan, "A general framework for a class of first order primal-dual algorithms for convex optimization in imaging science," *SIAM J. Imaging Sci.*, vol. 3, no. 4, pp. 1015–1046, 2010.

(a) Original Image

(b) reconstructed with TV, 26.83dB
$\mu = 0.42$, $\lambda = 0.06$

(c) reconstructed with SLTV, 27.03dB
$\mu = 0.32$, $\lambda = 1.3$, $\Omega = \Omega_4$.

Fig. 4. Joint demosaicking-denoising experiment on image 14 of the Kodak test base. The PSNR values correspond to the whole image, not to the crop selected here. The parameters μ and λ were empirically optimized to maximize the PSNR. 100 iterations of the algorithm were run.

[22] X. Zhang, M. Burger, and S. Osher, "A unified primal-dual algorithm framework based on Bregman iteration," *Journal of Scientific Computing*, pp. 1–27, 2010.

[23] P. L. Combettes and J.-C. Pesquet, "Proximal splitting methods in signal processing," in *Fixed-Point Algorithms for Inverse Problems in Science and Engineering*, H. H. Bauschke, R. Burachik, P. L. Combettes, V. Elser, D. R. Luke, and H. Wolkowicz, Eds. New York: Springer-Verlag, 2010.

[24] B. K. Gunturk, J. Glotzbach, Y. Altunbasak, R. W. Schaffer, and R. M. Mersereau, "Demosaicking: Color filter array interpolation," *IEEE Signal Processing Mag.*, vol. 22, no. 1, pp. 44–54, Jan. 2005.

[25] L. Condat, "Joint demosaicking and denoising by total variation minimization," GREYC, Tech. Rep. hal-00598807, Oct. 2010.